Estimation of permeable pathways and water content using tomographic radar data

S. S. HUBBARD, Lawrence Berkeley National Laboratory and University of California
J.E. PETERSON, JR, E. L. MAJER, P. T. ZAWISLANSKI, and K. H. WILLIAMS, Lawrence Berkeley National Laboratory, Berkeley, California
J. ROBERTS, Lawrence Livermore National Laboratory, Livermore, California
FRANK WOBBER, U.S. Department of Energy, Germantown, Maryland

Near-surface environmental investigations often require monitoring of the spatial distribution of water content and identification of preferential fluid flow paths. Water content estimates are needed, for example, to model and predict pollutant transport through the vadose zone and to subsequently design an efficient and reliable remediation plan. The characteristics of preferential flow paths, as well as the location and geometry of these features, are necessary to model and predict flow and transport in complex geological media such as fractured or strongly heterogeneous porous systems. Water content can be measured in the laboratory and in boreholes, and fracture zones are often identified from cores or borehole acoustic televiewer responses. However, these methods are costly, time-consuming, and invasive — all of which limit the ability to perform detailed and multidimensional vadose zone site characterization. Thus, there is a need to capture the spatial variations of these hydraulic parameters or features in an efficient and less invasive manner.

We investigate the use of dielectric information obtained from high resolution tomographic radar data for estimating subsurface water content and delineating distinct fluid flow paths in three case histories: one where data were collected at a single point in time and two where data were collected at the same locations but at different times. Processing the time-lapse radar data as "dielectric difference" cross-sections (measurements collected at an earlier time subtracted from those collected later) enhances subtle geophysical attribute changes due to dynamic processes such as steam flooding, infiltration tests, hydraulic fracturing, and the spread of contaminant plumes. In all case studies, the radar-assisted water content or fluid flow path estimates were confirmed by borehole measurements. The geophysical work at all three sites was supported by the Department of Energy, Office of Health and Environmental Research (DOE/OHER) under the Subsurface Science Program.

Table 1.

Material	Dielectric Constant
Sand (dry)	3-6
Sand (saturated)	20-30
Silts	5-30
Shales	5-15
Clays	5-40
Humid soil	30
Cultivated soil	15
Rocky soil	7
Sandy soil (dry)	3
Sandy soil (saturated)	19
Clayey soil (dry)	2
Clayey soil (saturated)	15
Sandstone (saturated)	6
Limestone (dry)	7
Limestone(saturated)	4-8
Basalt (saturated)	8
Granite (dry)	5
Granite (saturated)	7

Background. Ground penetrating radar (GPR) uses short pulses of high-frequency (10-1000 MHz) electromagnetic energy to probe the subsurface. Under favorable conditions, the radar signal traveltime is primarily affected by changes in the dielectric properties of the material which may be caused by variations in saturation, material constituency, material texture, temperature, and pore fluid composition. At radar frequencies, typical values for common geologic materials are 2-40 (Table 1). As the dielectric constant of water is 80 and air is 1, a material saturated with water has a higher dielectric constant than the same material in an unsaturated state.

GPR performance is often poor in electrically conductive environments such as systems saturated with saline water or dominated by clays; in general GPR performs best in unsaturated coarse- or moderately coarse-textured sediments and in some consolidated rocks such as granite. The three sites discussed here consist of clean sands, fractured basalts, and welded tuffs, respectively. When conditions are amenable to radar sounding and at the high frequencies used for data acquisition, the dependency of radar velocity on electrical conductivity is negligible and the radar signal velocity (V) can be related to the real part of the dielectric constant (κ) by the simple relationship $\kappa \approx (c/V)^2$ where c is the plane-wave propagation velocity of electromagnetic waves in free space; thus, dielectric constants can be estimated from GPR velocities.

Tomographic radar methods transmit electromagnetic energy directly from a transmitting antenna in one borehole to a receiving antenna in another borehole over several transmitting/receiving locations. Data reduction includes initially picking the arrival time (or traveltime) for all transmitter/receiver pairs. The interwell area is then discretized into rectangular cells of constant slowness (the reciprocal of velocity) and an attempt is made to determine the slowness within each cell such that the differences between the observed traveltimes and those calculated for a raypath passing through several nodes is a minimum for all raypaths. The procedures for collecting and processing radar data in the format necessary for velocity estimation are relatively new and still topics of research. Nonetheless, the increase in use of radar data for detailed site investigation suggests these procedures will become standardized. Obtaining information about radar propagation velocity is

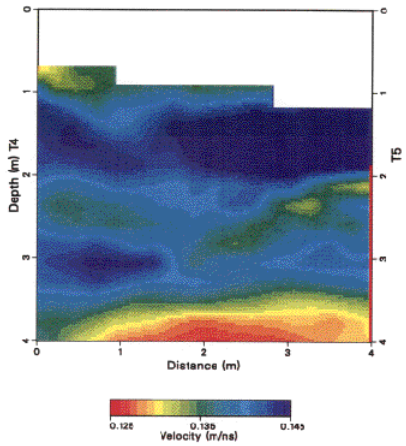

Figure 1. Velocity estimates for well pair T4-T5 obtained from inverting the crosshole radar data.

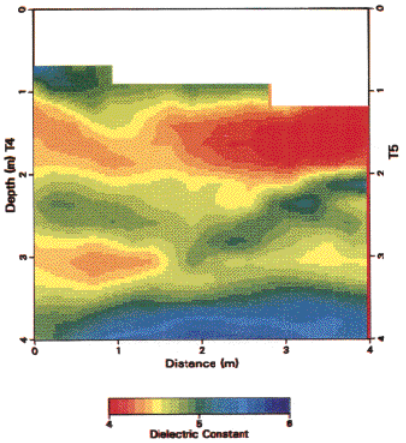

Figure 2. Dielectric estimates for well pair T4-T5 obtained using the velocity estimates in Figure 1.

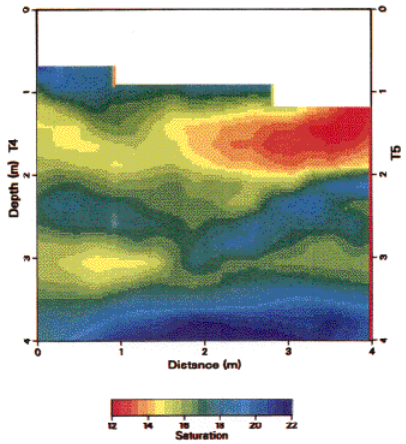

Figure 3. Saturation estimates for well pair T4-T5 obtained using the dielectric estimates shown in Figure 2 together with Topp's relation.

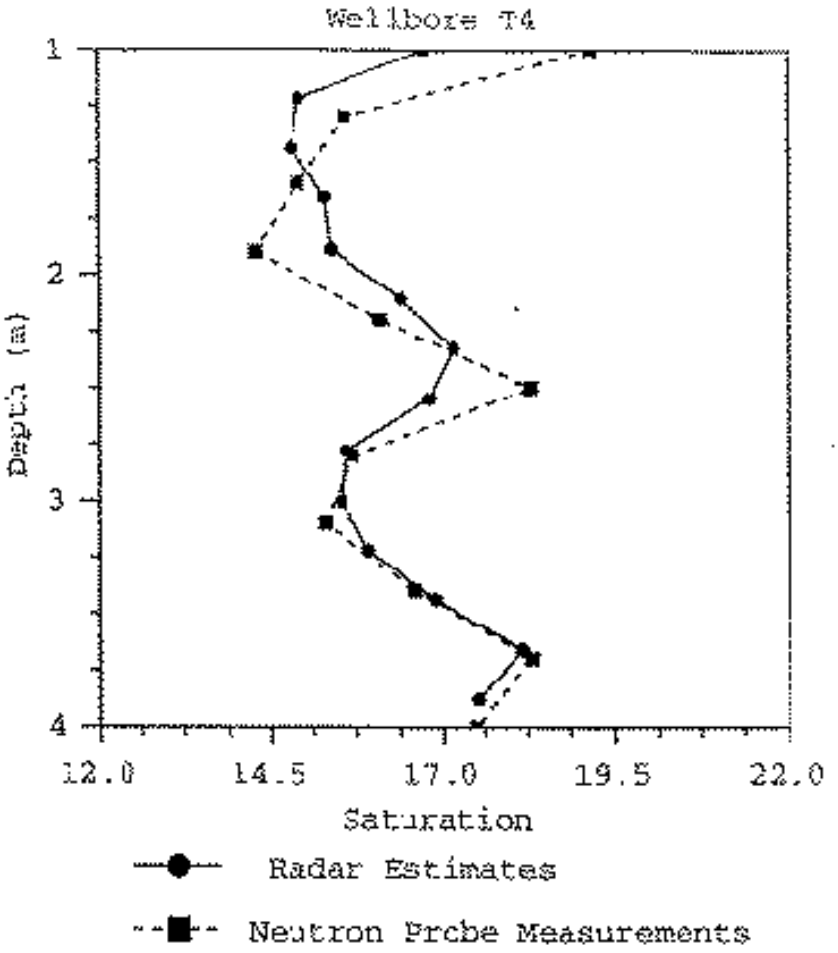

Figure 4. Comparison of saturation estimates at wellbore T4 obtained from neutron probe and tomographic radar data. The saturation estimates obtained from the radar data are remarkably similar to those collected using neutron probe data, and suggest that crosshole radar data can provide two-dimensional water saturation estimates.

beneficial since interval velocities can be related to a material's dielectric constant. This, in turn, can be used to estimate hydrogeological parameters or features.

Volumetric water content (θ) and saturation (S) are related by: $\theta = S \cdot \phi$ (ϕ = porosity). Both empirical and theoretical approaches have been used to investigate the relationship between dielectric constants and moisture content. Topp's well known petrophysical relation ($\theta = -5.3 \times 10^{-2} + 2.92 \times 10^{-2} K - 5.5 \times 10^{-4} K^2 + 4.3 \times 10^{-6} K^3$, G.C. Topp et al., *Water Resources Research*, 1980) suggests that dielectric constant increases with volumetric water content. Relationships between dielectric and hydraulic parameters can also be represented using mixture formulae, such as developed by Roth et al. in "Calibration of time domain reflectometry for water content measurement using a composite dielectric approach (*Water Resources Research*, 1990).

Roth's formula and Topp's regression relationship are widely used in soil physics studies to relate TDR measurements of dielectric constants to water content. These petrophysical relationships are not universal but they provide examples of how the dielectric constant obtained from tomographic radar data measurements can be used to estimate moisture content.

Processed time-lapse radar data yield estimates of the change in electromagnetic wave propagation velocities over some time period or (by the mathematical means previously described) the change in dielectric constants. Data collected as the saturation state varies (e.g., during an infiltration test) will reveal changes in dielectric constants caused by water content variations.

In fractured or strongly hetero-

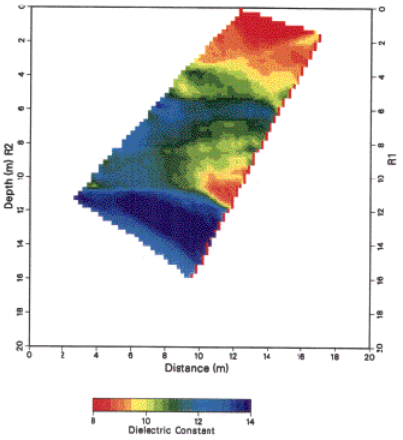

Figure 5a. Dielectric estimates for well pair R1 -R2 inferred using information from crosshole radar data collected prior to infiltration experiment.

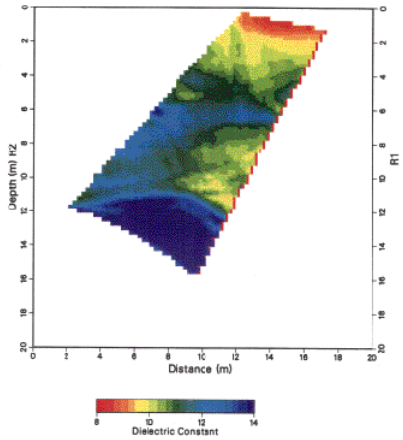

Figure 5b. Dielectric estimates for well pair R1-R2 inferred using information from crosshole radar data collected nine days after infiltration began.

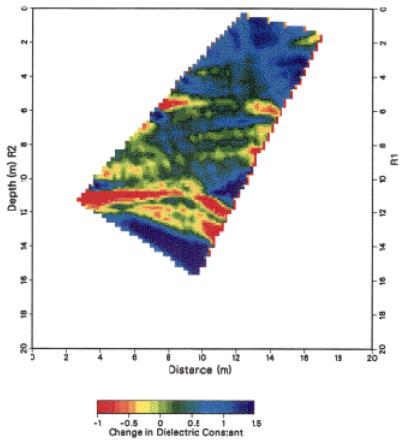

Figure 5c. Difference in dielectric constants between data collected prior to infiltration and after infiltration began. The linear features are interpreted to be water-conducting fracture zones.

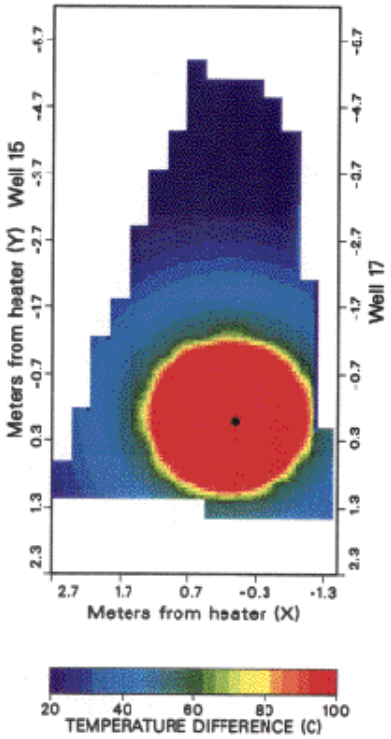

Figure 6. Difference in interpolated borehole temperature measurements prior to application of heat and those collected five months after the test began. The black dot indicates the heater location.

geneous porous media, the greatest dielectric constant changes will occur during infiltration within interconnected high permeability layers or features, and thus the radar "difference" data can illuminate these preferential flow paths.

Saturation estimation using tomographic radar data. The impetus for this study was the hydrogeologic characterization of the DOE's Subsurface Program Bacterial Transport Site in Oyster, Virginia, where the near subsurface consists of unconsolidated gravelly sand sediments. As the sediments are moderately homogeneous and no changes in subsurface temperature or pore fluid composition are expected, the radar response in the vadose zone should be largely controlled by variations in saturation. Three tomographic profiles were collected in one day at depths of 0.5-11 m. Boreholes were separated by 4 m. Antenna spacing within the wellbore was 0.25 m. The transmitting antenna for well pair T4-T5 was in hole T4 and the receiving antenna in hole T5. A PulseEKKO 100 system, with 100 Mhz central frequency borehole antennas, was employed at this site and the other two sites discussed later.

Slownesses were estimated for this study (as well as for the following two data sets) using a straight-raypath algebraic reconstruction inversion technique. Figure 1 shows the velocities obtained from the slowness values. The electromagnetic propagation velocity range of approximately 0.125-0.145 m/ns is typical for unsaturated, unconsolidated sands. These velocities were transferred into dielectric constant estimates (Figure 2). The dielectric constant estimates were converted to water content estimates and then into saturation with a constant porosity value of 0.4 obtained from averaged core measurements. These estimates (Figure 3) suggest the presence of subsurface horizontal layers with varying saturations and a vertical and horizontal resolution of approximately 0.20 m.

We compared these saturation estimates measurements with neutron probe measurements in the wellbores. These were collected from the surface to the water table every 15-30 cm using a CPN 503DR Hydroprobe. When high energy neutrons from the neutron probe are emitted into the formation, they collide with other nuclei and lose energy, or become thermalized. Of all common nuclei present in earth materials, hydrogen is the most effective neutron moderator because its mass is nearly equal to that of a neutron. In soil and rock environments which do not contain hydrocarbons, water is by far the largest reservoir of hydrogen, making neutron attenuation particularly useful for moisture detection. Although formation-specific calibration of neutron counts is necessary for precise quantification of moisture content, estimates of saturation may be obtained by using the ratio of thermal neutron counts at any depth to those measured under saturated conditions. As there are only minor variations in formation mineralogy and bulk density in the Oyster sediments, the saturation-neutron count relationship was assumed to be linear, and this was used to estimate saturation as a function of depth. Figure 4 compares the neutron probe estimates of saturation at well T4 with the estimates obtained using tomographic radar. Correlation is excellent, and suggests tomographic radar methods are extremely use-

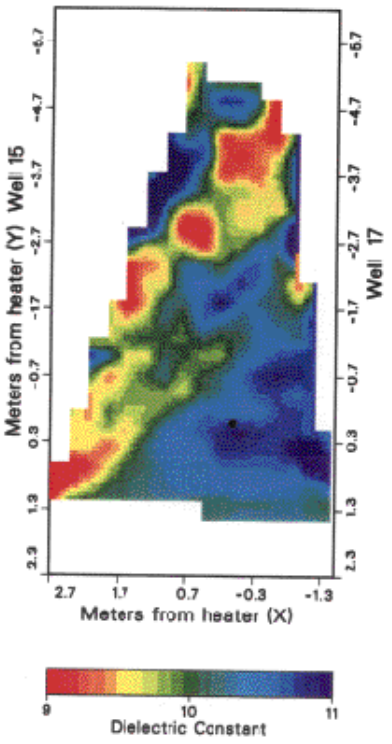

Figure 7a. Dielectric constant estimates for well pair 15-17 inferred using information from crosshole radar data collected prior to heat application.

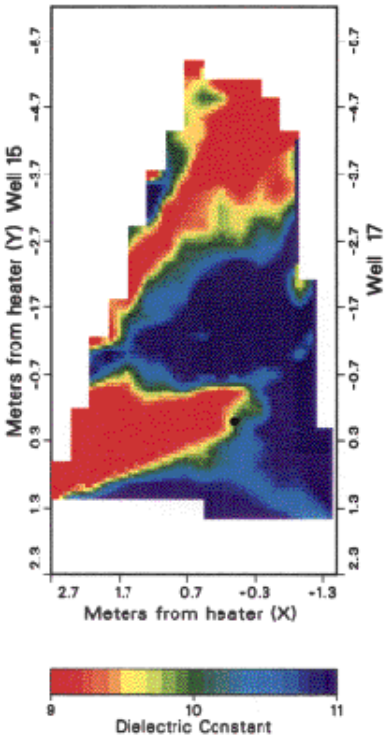

Figure 7b. Dielectric constant estimates for well pair 15-17 inferred using information from crosshole radar data collected after heat had been applied for five months.

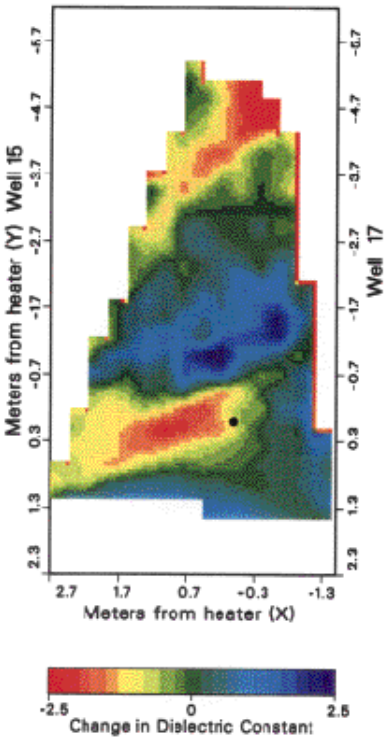

Figure 7c. Difference in dielectric constants from data collected prior to heat application and after heat had been applied for five months.

ful for estimating two-dimensional water saturation in fairly homogeneous environments.

Delineation of permeable pathways using time-lapse tomographic radar. Radar data were collected at the Box Canyon Site in Idaho to aid near-suface fracture and rock characterization. The subsurface is a "clean" analog to contaminated subsurface at the nearby Idaho National Engineering Laboratory. Both consist of Snake River Plain Quaternary fractured and vesicular basalt flows interlayered with sedimentary deposits. Fracture orientation is random and fracture thickness varies from microscopic to a few centimeters. These fractures were formed during basalt cooling and often form permeable pathways. Additionally, high horizontal permeable pathways are present as "rubble zones" which form at the top of the basalt flows during lava cooling. Fracture and rubble zones are believed the major conduits for fluid flow; to predict and control contaminant transport through the fractured Snake River Plain vadose zone, an understanding of the nature and connectivity of these preferential flow paths is essential.

Four tomographic radar profiles were collected prior to and during an infiltration test at Box Canyon. The infiltration test imposed a hydraulic head above the ground surface within an enclosed barrier, and falling head and subsurface responses were monitored as a function of time. Radar data were collected one month before and nine days after the infiltration test began. Wellbore spacing was 4.5 m. Data were collected at approximately 0.5-15 m with antenna spacing of 0.25 m.

Data were inverted for slownesses, converted to electromagnetic wave propagation velocities, and then to dielectric constants. Examples of the dielectric constant estimates for profiles before and after commencement of the infiltration test are shown in Figure 5a and 5b, respectively. As the subsurface geology and temperature remain constant, the differences (Figure 5c) between these figures are attributed solely to variations in saturation due to water infiltration. These "difference" data reveal that the dielectric constants increase on average 4% during infiltration, and that changes as high as 20% occur locally. The increases in dielectric constants near the surface and along permeable pathways are interpreted to be due to an increase in saturation associated with the infiltration test. We did not attempt to estimate the change in water content, but instead used the differences in dielectric constant to infer the presence of preferential fluid flow paths. For example, Figure 5c reveals a linear (blue) feature extending from 6 m below ground in well R2 downward to approximately 12 m in R1. The increase in dielectric constant along this lineament is interpreted to be caused by increased wetting of a fracture zone. This lineament intersects R2 at a location where a borehole camera reveals a fracture swarm, and extension of this lineament to another borehole 5 m away intersects a portion of the core where a 1.5 cm fracture was identified. Several other linear features are also identifiable on the difference section at depths of 6-12 m; these are interpreted to be part of a pervasive subhorizontal fracture swarm that is apparent from borehole camera data as well as at a nearby outcrop. These

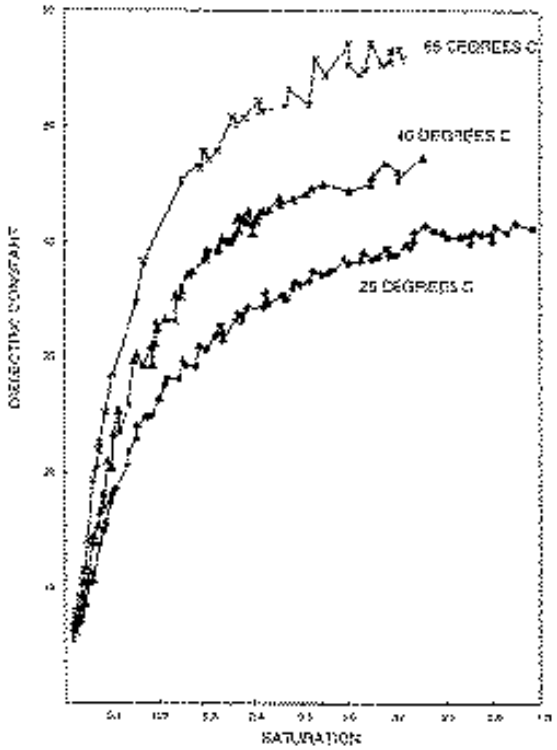

Figure 8. Laboratory dielectric measurements made at 100 kHz as a function of saturation and temperature. These data suggest that dielectric constants increase with both saturation and temperature.

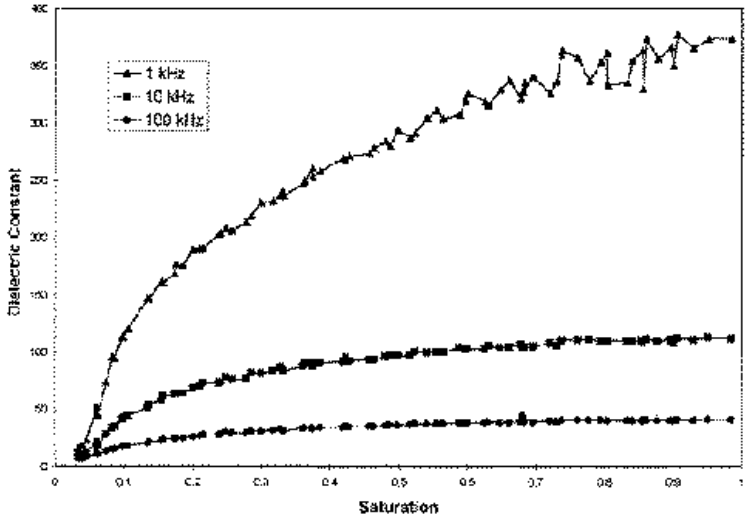

Figure 9. Laboratory dielectric measurements made at 23° C as a function of saturation and frequency. The dispersive nature of the dielectric constant renders it difficult to use a petrophysical model inferred from the 100 kHz laboratory data to predict changes in saturation using 100 MHz field data.

results exemplify the use of tomographic time-lapse radar data for aiding characterization and imaging of permeable flow zones.

Monitoring water distribution using time-lapse tomographic radar. Tomographic radar data were collected in time-lapse manner to monitor water distribution at the Yucca Mountain Single Heater Test Site in the thermomechanical alcove of the Exploratory Studies Facilities (ESF) thermal test facility at the Yucca Mountain Repository. Numerous geophysical hydrological and geochemical investigations have been and are being performed to gain an understanding about coupled processes including fluid movement; this information will become part of a comprehensive database to determine if the site is appropriate for nuclear waste storage. At the Single Heater Test Site, the application of heat over time is expected to progressively drive moisture away from the heater. The subsurface consists of the welded Topopah Spring Tuff, which has primary porosity of approximately 11% and fracture spacing of 2-4 per meter.

Two crosshole tomographic radar profiles were collected prior to the heater test and five months after it began. The boreholes were not parallel and radar wellbore separations varied along the length of the borehole from 1-4 m. Antenna spacing in the wellbores was 0.25 m. The differences between the initial constant subsurface temperature of 25° C and the temperature distribution five months after the test began were obtained from probes installed along the boreholes. These temperature differences are shown in Figure 6. The heater location is annotated by a black dot.

As in the other cases, data were inverted for slownesses, converted to velocities, and finally converted to dielectric constants. Profile 15-17, collected prior to heat application, is shown in Figure 7a and the same profile, collected five months after the test commenced, is shown in Figure 7b. The dielectric constant differences are shown in Figure 7c. Unlike the infiltration test, both saturation and temperature vary during this experiment, and thus the variations in dielectric constant can not be used directly to infer the change in saturation. The relationship between dielectric constant, saturation and temperature must be known to estimate the change in saturation. To investigate these relationships, laboratory measurements of the dielectric constant as a function of both saturation and temperature were performed on disk-shaped core samples with diameters of 5.1 cm and a diameter-to-thickness aspect ratio of >10:1. These measurements were made at 23°, 40° and 65° C, over a saturation range of 0-100% during wetting and drying experiments as well as at various frequencies, the highest of which was 100 kHz. Figure 8 shows an example of the laboratory dielectric measurements obtained during a wetting experiment with 100 kHz signal. This figure reveals that for the Yucca Mountain Topopah Spring Tuff, the dielectric constants increase with increasing saturation *and* temperature.

We originally intended to use the data in Figure 8 to obtain a relationship between the logarithm of saturation, temperature and dielectric measurements which would enable us to estimate interwell saturation given the radar dielectric constant differences (Figure 7c) and the bore-

hole temperature measurement differences (Figure 6). However, the dispersive nature of dielectric constants at frequencies lower than 10 MHz for materials with electrical conductivities less than 100 mS/m prohibited us from using a relation modeled from these 100 kHz laboratory measurements to predict saturation given the 100 MHz radar dielectric constant measurements. The effect of frequency on the dielectric constant is displayed in Figure 9, which shows the dielectric and saturation laboratory measurements collected at a constant temperature of 23° C at various frequencies. This reveals that dielectric constants decrease with increasing frequency; for comparison, our 100 MHz radar dielectric constant estimates fall in the range of 8-12.

An alternative method of relating dielectric constant to saturation and temperature is to perform regression analysis using dielectric constant estimates obtained from crosshole radar data along with borehole measurements of saturation obtained from neutron logs and borehole temperature measurements. This work is currently in progress, and we expect that this method will produce a dielectric constant-saturation-temperature relationship that can be used with radar data to estimate the two-dimensional change in saturation.

Although we can not presently estimate the change in saturation at the Single Heater Test Site, some qualitative statements can be made about subsurface conditions using the dielectric constant differences. For example, this "difference" profile (Figure 7c) reveals that the dielectric constants have decreased near the heater, which suggests that temperature or saturation, or both, have decreased over time. Because we know that the temperature has only increased near the heater in the time during the acquisition of the two data sets, we can infer drying in the vicinity of the heater, and that the drying is not symmetric but is likely controlled by the rock heterogeneity. However, the increase in dielectric constant shown by the blue zone in the middle of Figure 7c can be caused by an increase in saturation, temperature, or both, and since we know that the temperature has increased over time, it is impossible to estimate the variations in saturation without incorporating petrophysical information. LE

Corresponding author: Susan Hubbard, shubbard@csc.lbl.gov